Plant, Cell & Environment

Plant, Cell and Environment (2015) **38**, 655–669 doi: 10.1111/pce.12428

Original Article

Physiological and proteomic analyses of salt stress response in the halophyte *Halogeton glomeratus*

Juncheng Wang[1,2]*, Yaxiong Meng[1,2]*, Baochun Li[1,3], Xiaole Ma[1,2], Yong Lai[1,2], Erjing Si[1,2], Ke Yang[1,2], Xianliang Xu[1,2], Xunwu Shang[1], Huajun Wang[1,2] & Di Wang[1,2]

[1]*Gansu Provincial Key Lab of Aridland Crop Science/Gansu Key Lab of Crop Improvement & Germplasm Enhancement, Lanzhou 730070, China and* [2]*College of Agronomy and* [3]*College of Life Sciences and Technology, Gansu Agricultural University, Lanzhou 730070, China*

ABSTRACT

Very little is known about the adaptation mechanism of Chenopodiaceae *Halogeton glomeratus*, a succulent annual halophyte, under saline conditions. In this study, we investigated the morphological and physiological adaptation mechanisms of seedlings exposed to different concentrations of NaCl treatment for 21 d. Our results revealed that *H. glomeratus* has a robust ability to tolerate salt; its optimal growth occurs under approximately 100 mM NaCl conditions. Salt crystals were deposited in water-storage tissue under saline conditions. We speculate that osmotic adjustment may be the primary mechanism of salt tolerance in *H. glomeratus*, which transports toxic ions such as sodium into specific salt-storage cells and compartmentalizes them in large vacuoles to maintain the water content of tissues and the succulence of the leaves. To investigate the molecular response mechanisms to salt stress in *H. glomeratus*, we conducted a comparative proteomic analysis of seedling leaves that had been exposed to 200 mM NaCl for 24 h, 72 h and 7 d. Forty-nine protein spots, exhibiting significant changes in abundance after stress, were identified using matrix-assisted laser desorption ionization tandem time-of-flight mass spectrometry (MALDI-TOF/TOF MS/MS) and similarity searches across EST database of *H. glomeratus*. These stress-responsive proteins were categorized into nine functional groups, such as photosynthesis, carbohydrate and energy metabolism, and stress and defence response.

Key-words: EST database; physiology; proteomic; salinity; tolerance.

INTRODUCTION

Soil salinity is a significant abiotic stress that limits the distribution and productivity of crops worldwide (Zhu 2000; Tuteja 2007; Munns & Tester 2008). High concentrations of salt lead to an ionic imbalance, hyperosmotic stress and nutrient deficiency in plants (Zhu 2001; Flowers 2004). Improving the salt tolerance of crops and managing the soil salinity are necessary to meet the increasing food supply demands worldwide (Yang *et al.* 2012; Barkla *et al.* 2013). The effects of salt stress can limit plant growth and development and can even lead to plant's death (Aoki *et al.* 2005). Coping with salt stress involves complicated mechanisms that include developmental, morphological, physiological and biochemical strategies (Taji *et al.* 2004). Further, salt stress-regulation genes are expressed, which leads to changes in the protein profile that help plants to adapt to salt accumulation (Parker *et al.* 2006). Many salt-responsive genes, which are involved in membrane transport, signal transduction, redox reactions and other processes, play important roles under salt stress conditions (Zhang *et al.* 2008). Previous research suggested that halophytes possess more salt tolerance-related genes than glycophytes (Askari *et al.* 2006; Yu *et al.* 2011; Bartels & Dinakar 2013). Halophytes, which account for approximately 1% of the world flora, naturally survive to reproduce in saline soil. These plants have evolved various regulatory and metabolic mechanisms to cope with soil salinity, such as growth and osmotic adjustment and regulation of ion uptake and transport (Flowers & Colmer 2008). Proteomics is widely used to study protein profiles of plants experiencing stress conditions (Hossain *et al.* 2011), and proteomics has contributed to the identification of specific functions of genes and proteins involved in salt tolerance of halophytes. Some of these salt tolerance genes have been cloned from halophytes and then transferred to rice, alfalfa, tobacco, *Arabidopsis* and other glycophytes in an attempt to improve salt tolerance. These genes include *AlSAP* (a gene encoding for an A20/AN1 zinc-finger protein) (Saad *et al.* 2010), *NHX* (a Na^+/H^+ antiporter gene) (Ohta *et al.* 2002; Wu *et al.* 2009; Guan *et al.* 2011), *SOS1* (a gene encoding a plasma membrane Na^+/H^+ antiporter) (Yadav *et al.* 2012) and *H^+-PPase* (an H^+-pyrophosphatase gene) (Gao *et al.* 2006; Guo *et al.* 2006). Some salt stress-related proteomic analyses have already been conducted, but these studies only focus upon a few halophytes, including *Aeluropus lagopoides* (Sobhanian *et al.* 2010), *Suaeda aegyptiaca* (Askari *et al.* 2006), *Salicornia*

Correspondence: H. Wang. Fax: +86-0931-7631145; e-mail: whuajun@yahoo.com

*These authors contributed equally to this work.

Conflict of interest: The authors declared that they have no competing interests.

europaea (Wang *et al*. 2009; Fan *et al*. 2011), *Cakile maritime* (Debez *et al*. 2012) and *Thellungiella halophila* (Wang *et al*. 2013a). Because protein identifications rely upon sequence similarity to homologous proteins in databases, proteomics research in unsequenced species is largely limited due to the lack of genomic information (Habermann *et al*. 2004; Renard *et al*. 2012). However, proteomics is still a powerful approach to study non-model species (Carpentier *et al*. 2008). In non-model species, mass spectrometry (MS) identification of unknown proteins is carried out by matching sequences available in similar evolutionary origin, or at the higher level, and even the whole database, and this identification method has been widely recognized (Sobhanian *et al*. 2010; Li *et al*. 2011; Sinha & Chattopadhyay 2011; Yu *et al*. 2011; Debez *et al*. 2012). Moreover, with the development of next-generation sequencing technologies, the achievement of available nucleotide, EST and protein sequences in non-model plant species is increasing, and the number of identified proteins and data reliability are improved significantly (Champagne & Boutry 2013). The identified salt-responsive proteins participate in diverse functional categories, such as photosynthesis, reactive oxygen species (ROS) scavenging systems, osmotic homeostasis, signal transduction, ion homeostasis and cross-membrane transport, protein fate, cytoskeleton dynamics and cross-tolerance to multiple stresses (Zhang *et al*. 2011). Halophytes employ systematic mechanisms to improve salt tolerance under salt stress conditions. Identification of these mechanisms will better characterize the phenomenon of salinity tolerance and will direct approaches to improve the salinity tolerance of crops (Hossain *et al*. 2011).

Halogeton glomeratus (Chenopodiaceae) is a succulent annual halophyte and is one of the most widely distributed halophytes in Central Asia and arid regions in northwestern China. This species was introduced into the America in 1934 and rapidly spread into Western states (Dayton 1951; Duda *et al*. 2003). The plant has high concentration of oxalates, which can be poisonous to grazing animals, particularly for sheep (Dye 1956; James & Butcher 1972). *H. glomeratus* grows in saline soils in arid and semi-arid regions. It was reported to have a high tolerance to NaCl at germination stage, being able to still germinate in 1000 mM NaCl (Khan *et al*. 2001), and the secondary tissues of the stem and root appear to be two distinct structural patterns as the products of successive, extrafascicular and bidirectional cambia of varying circumference (Baird & Blackwell 1980). However, little is known about the physiological and molecular adaptive mechanism of tolerance to salt in this halophyte. For this study, we analysed the salt tolerance of *H. glomeratus* under 0, 100, 200, 300, 400 and 500 mM NaCl conditions for 3 weeks using physiological approaches. We also investigated the response of the proteome to salt stress using a comparative proteomic study of plants exposed to 200 mM NaCl conditions for 24 h, 72 h and 7 d. We identified 49 protein spots that changed their abundance significantly and reviewed their roles in adaptation of *H. glomeratus* to salt conditions. These results lay a basis for further investigation of the salt tolerance mechanisms of *H. glomeratus*.

MATERIALS AND METHODS

Plant growth and salt treatments

Seeds of *H. glomeratus* were collected from a salinized river shoal located in Huining, Gansu Province, China. Seeds were sown in plastic pots (11 cm in diameter and 10 cm in height) filled with a mixture of sand and vermiculite (1:1 v/v). Plants were raised in a growth chamber under a 16 h light/8 h dark cycle at temperatures of 25 °C/18 °C and relative humidities of 60%/80%, respectively. Irradiation intensity was approximately 300 μmol m^{-2} s^{-1}. The plants were irrigated daily with half-strength Hoagland's solution.

After 2 months, the seedlings were treated with half-strength Hoagland's solution containing different concentrations of NaCl for 21 d. To avoid salt shock injuries, salt concentrations were increased in 100 mM d^{-1} increments until final concentrations (100, 200, 300, 400 and 500 mM NaCl) were achieved. Control plants were maintained in half-strength Hoagland's solution without NaCl. Salt solutions were changed every day to maintain stable NaCl concentrations and avoid nutrient deficiency. After salt treatment, the leaves were harvested from control and salt-treated plants for physiological and anatomical analyses.

In a separate experiment, 2-month-old seedlings were treated with half-strength Hoagland's solution containing 200 mM NaCl for 24 h, 72 h and 7 d. A control group of plants was maintained in half-strength Hoagland's solution without NaCl. Leaves were harvested immediately at 0900 h when each treatment was completed, frozen in liquid nitrogen and maintained at −80 °C until proteomic analysis, and three independent experiments were performed as biological replicates.

Leaf microstructure analysis and observation of salt crystals

Anatomical features of the roots, stems and leaf tissues were treated with a safranin and fast-green stain procedure according to the methods of Schuerger *et al*. (1997). Fresh leaves treated with different NaCl concentrations were mounted on double-sided thick adhesive tape adhered to metal stubs used for scanning electron microscopy (SEM) of each leaf surface. The leaf abaxial surfaces were scanned with a SEM (S-3400N, Hitachi Group Company, Tokyo, Japan) with 3.0 kV current and 60 Pa pressure.

We also observed salt crystals in the leaves of salt-treated plants. Firstly, fresh leaves from different salt treatment groups were placed in mortars and immediately frozen in liquid nitrogen. The leaf samples were then transferred to a freeze dryer for 24 h at −55 °C to remove all the water from the leaves. Freeze-dried leaves were cross-cut at an approximately 60-degree angle gradient. Cross-cuts were analysed by a SEM as described earlier.

Physiological analyses of seedlings

The fresh weight (FW) of each plant was measured immediately after harvesting, and the dry weight (DW) was

determined after drying at 80 °C until the weight was maintained. Tissue water content (TWC) was calculated according to the following formula: (FW – DW)/FW × 100%. Each measurement was conducted five times for each treatment group.

To determine the potassium and sodium contents of the leaves, leaf samples were dried for 15 min at 105 °C. The samples were then dried in an 80 °C oven until a constant weight was maintained for each leaf. Then, dried leaves were ashed in an oven at 500 °C and extracted with HNO_3. Ion contents of the leaves were measured using an atomic absorption spectrophotometer (AA240; Varian Medical Systems, Palo Alto, CA, USA).

Protein extraction from the leaves

We extracted total proteins from leaves exposed to salt treatments for different lengths of time (200 mM NaCl for 0 h, 24 h, 72 h and 7 d) according to the method described by Li *et al*. (2011), with modifications. Frozen leaf tissue was ground in liquid nitrogen to a fine powder and incubated in ice-cold extraction buffer [10% (w/v) tricarboxylic acid (TCA) in acetone with 0.07% (v/v) β-mercaptoethanol] overnight at –20 °C. Homogenates were centrifuged at 20 000 *g* for 30 min at 4 °C. The pellets were washed with cold acetone containing 0.07% β-mercaptoethanol, incubated at –20 °C for 1 h and centrifuged at 20 000 *g* for 20 min at 4 °C. The process was repeated two or three times until the supernatant was colourless. Next, the pellets were washed twice with ice-cold 80% acetone containing 0.07% β-mercaptoethanol and centrifuged as described earlier and then the pellets were dried by vacuum. The remaining pellets were dissolved in a solubilization buffer [7 M urea, 2 M thiourea, 65 mM dithiothreitol (DTT), 4% (w/v) CHAPS (3-[(3-Cholamidopropyl)dimethylammonio]-1-propanesulfonate)] at room temperature for 2 h and then centrifuged at 20 000 *g* for 30 min at 4 °C. The protein concentration of each pellet was determined according to the method described by Peterson (1977). Bovine serum albumin (BSA) was used as a standard.

Two-dimensional gel electrophoresis (2-DE) and image analysis

For isoelectric focusing (IEF) in the first dimension, protein samples were dissolved in rehydration buffer containing 7 M urea, 2 M thiourea, 4% (w/v) CHAPS, 65 mM DTT, 0.001% (w/v) bromophenol blue and 0.2% (w/v) ampholytes (pH 3–10) (Bio-Lyte; Bio-Rad, Hercules, CA, USA). Next, 1000 μg of protein samples was loaded into an IPG strip holder. Immobilized linear gradient strips (pH 4–7, 18 cm; Bio-Rad) were rehydrated at 50 V for 14 h at 20 °C. Electrofocusing was performed using a Protean IEF cell system (Bio-Rad) at 20 °C using a four-step process: 250 V for 1.5 h with a rapid ramp; 1000 V for 2.5 h with a linear ram; 9000 V for 5 h with a linear ramp; and 9000 V for 90 000 V-h with a rapid ramp. After IEF, the strips were incubated for 15 min in equilibration buffer I [6 M urea, 2% sodium dodecyl sulphate (SDS), 0.375 M Tris–HCl (pH 8.8), 20% glycerol and 130 mM DTT]. The strips were then incubated in equilibration buffer II [6 M urea, 2% SDS, 0.375 M Tris–HCl (pH 8.8), 20% glycerol and 135 mM iodoacetamide] for 15 min.

The second dimension separation of proteins was performed on a 12.5% polyacrylamide SDS gel using a Bio-Rad electrophoresis kit (Bio-Rad). Gels were stained with CBB G-250. The 2-DE gels were scanned using a UMAX PowerLook 2100XL scanner (Power Company, Chinese Taipei). A total of 12 2-DE gels were analysed using PDQuest software (version 8.0.1; Bio-Rad). To compensate for subtle differences in sample loading, gel staining and destaining, the volume of each spot was normalized as a percentage of the total volume of all the spots present in the gel. Manual inspection and editing were conducted to verify the auto-detected and matched results. Spots with more than a twofold change between the control and treatment samples were analysed by Student's *t*-test, and $P < 0.05$ was considered to indicate significant changes in abundance.

Protein spots were selected for profile analysis only if they were confirmed to have a consistent level of abundance in three independent sample sets.

Protein identification and database searching

Protein spots that exhibited reproducible changes between the control and treatment samples were excised from the gels and digested with trypsin, based upon the procedure described by Sheffield *et al*. (2006). MS and tandem mass spectrometry (MS/MS) data for protein identification were obtained by using a matrix-assisted laser desorption ionization time-of-flight (MALDI-TOF/TOF) instrument (4800 Plus MALDI TOF/TOF™ Analyzer; AB SCIEX, Framingham, MA, USA) as previously described by Tada & Kashimura (2009). The MS/MS spectra search was performed using MASCOT search engine (version 2.2, Matrix Science, London, UK) to search the EST database of *H. glomeratus* (containing 29 245 sequences) with the following parameter settings: 100 ppm precursor tolerance, trypsin cleavage (one missed cleavage allowed), carbamidomethylation set as fixed modification, oxidation of methionine allowed as a variable modification and MS/MS fragment tolerance set to 0.4 Da. A protein confidence index ≥95% was used for further manual validation. For a confident identification, the criteria used were as follows: the identified protein had a significant hit, the protein score at least 69, the coverage of protein sequence by matching peptides at least two, and there were at least 10% peptide sequence matches above the identity threshold (Table 1 and Supporting Information Table S2). The EST database of *H. glomeratus* was constructed using the following steps: *de novo* transcriptome sequencing of *H. glomeratus* detected 50 275 unigenes (all sequence data have been deposited in the National Center for Biotechnology Information and is accessible in BioProject ID PRJNA 254029; 2 July 2015 release), and all assembled unigenes were firstly aligned by blastx (*E*-value <0.00001) to protein databases in the priority order of nr, Swiss-Prot, KEGG and COG. Unigenes aligned to a higher priority database would not be aligned to

Table 1. Identification and analysis of proteins that were up-regulated and down-regulated in response to salt stress in leaves of *Halogeton glomeratus*

Functional category (*n*) Spot No.[a]	Protein name[b]	Plant species[c]	Accession No.[d]	Thr. MW (kDa)/pI[e]	Score[f]	Cov (%)[g]	PM[h]	Cellular location[i]	Fold change[j] Ratio ± SE 24 h	72 h	7 d
Photosynthesis (11)											
3↑	Ribulose bisphosphate carboxylase small chain 1, chloroplastic (RuBisCO small subunit 1)	*Mesembryanthemum crystallinum*	Unigene1053_All	20 462.1/8.94	70	42	8	Chlo	NDC	0.90 ± 0.11	0.69 ± 0.14
9↑	Ribulose-1,5-bisphosphatecarboxylase/oxygenase large subunit (RBCOLSU)	*Phaulothamnus spinescens*	CL2339.Contig1_All	53 119.6/6.22	90	30	10	Cyto	NDC	2.18 ± 0.30	1.07 ± 0.19
12↑	Oxygen-evolving enhancer protein 1, chloroplastic (OEE1)	*Populus trichocarpa*	Unigene3658_All	35 450.1/7.52	265	56	12	Chlo	2.17 ± 0.17	2.21 ± 0.35	2.7 ± 0.22
14↑	Ribulose-1,5-bisphosphatecarboxylase/oxygenase small subunit (RuBisCO small subunit)	*Mesembryanthemum crystallinum*	Unigene7349_All	13 598.6/7.71	120	33	4	Chlo	NDC	1.58 ± 0.33	2.96 ± 0.47
17↓	Phosphoribulokinase, chloroplastic (PRKase)	*Spinacia oleracea*	Unigene25793_All	46 351.3/5.75	604	58	15	Chlo	0.63 ± 0.12	0.59 ± 0.08	0.38 ± 0.09
28↓	Transketolase, chloroplastic (TK)	*Spinacia oleracea*	Unigene3714_All	80 487.8/6.18	514	54	28	Chlo	0.31 ± 0.05	0.46 ± 0.05	0.21 ± 0.04
29↑	Ribulose bisphosphate carboxylase small chain 1, chloroplastic (RuBisCO small subunit 1)	*Mesembrya*	Unigene1053_All	20 462.1/8.94	432	66	12	Chlo	2.56 ± 0.35	1.79 ± 0.23	1.51 ± 0.18
36↑	Ribulose-1,5-bisphosphate carboxylase/oxygenase small subunit (RuBisCO small subunit)	*Mesembryanthemum crystallinum*	Unigene7349_All	13 598.6/7.71	134	38	4	Chlo	1.84 ± 0.22	1.58 ± 0.28	1.47 ± 0.12
37↓	Sedoheptulose-1,7-bisphosphatase, chloroplastic (SED(1,7)P2ase)	*Spinacia oleracea*	Unigene20638_All	42 725.6/5.81	672	52	23	Chlo	0.42 ± 0.06	0.69 ± 0.13	0.41 ± 0.07
38↓	Transketolase, chloroplastic (TK)	*Spinacia oleracea*	Unigene3714_All	80 487.8/6.18	640	54	27	Chlo	0.52 ± 0.09	0.38 ± 0.06	0.24 ± 0.03
49↑	Beta carbonic anhydrase 2 (BCA2)	*Mesembryanthemum nodiflorum*	CL1219.Contig7_All	28 557.6/6.9	134	37	11	Cyto	1.55 ± 0.21	0.63 ± 0.06	1.70 ± 0.27
Carbohydrate and energy metabolism (5)											
4↑	NAD(P)H-quinone oxidoreductase subunit M, chloroplastic (NDH-1 subunit M)	*Vitis vinifera*	Unigene3073_All	24 461.9/5.2	278	66	10	Chlo	1.55 ± 0.19	2.02 ± 0.24	3.25 ± 0.32
8↑	ATP synthase subunit beta	*Medicago truncatula*	CL1360.Contig2_All	15 216/5.44	308	62	7	Cyto	2.60 ± 0.49	3.07 ± 0.65	3.57 ± 0.36
22↑	Triosephosphate isomerase, chloroplastic (TIM)	*Spinacia oleracea*	Unigene20753_All	34 555.6/5/90	187	53	12	Chlo	3.01 ± 0.32	3.80 ± 0.29	1.68 ± 0.19
26↓	NADP-dependent malic enzyme (NADP-ME)	*Hylocereus undatus*	Unigene14432_All	68 789.7/5.65	843	48	22	Cyto	0.21 ± 0.02	0.42 ± 0.4	0.36 ± 0.03
43↑	PREDICTED: lactoylglutathione lyase-like	*Glycine max*	Unigene9230_All	25 496.6/6.49	576	57	17	Chlo	2.39 ± 0.23	2.31 ± 0.19	2.20 ± 0.18
Translation and transcription (5)											
1↑	Elongation factor 1-delta (eEF-1B beta)	*Beta vulgaris subsp. vulgaris*	CL5216.Contig1_All	25 181.6/4.43	349	52	14	Cyto	1.38 ± 0.23	2.01 ± 0.43	0.92 ± 0.15
7↑	Nuclear transport factor, putative (NTF)	*Ricinus communis*	Unigene18485_All	13 612.6/5.37	270	57	5	Nucl	3.31 ± 0.53	1.17 ± 0.13	1.06 ± 0.20
18↓	Ribosomal protein S1, chloroplastic	*Spinacia oleracea*	Unigene23482_All	45 199.3/5.39	780	52	22	Chlo	0.50 ± 0.09	0.69 ± 0.10	0.33 ± 0.04
39↓	Eukaryotic translation initiation factor 5A2 (eIF 5A2)	*Tamarix androssowii*	Unigene6754_All	17 578.7/5.60	411	70	11	Cyto	0.55 ± 0.11	0.48 ± 0.07	0.39 ± 0.06
47↑	Transcription factor BTF3	*Zea mays*	Unigene9200_All	17 690.2/6.62	491	41	7	Cyto	2.52 ± 0.31	2.16 ± 0.60	0.87 ± 0.18
Amino acid metabolism (4)											
19↑	Plastid glutamine synthetase 2 (GS 2)	*Spinacia oleracea*	Unigene1393_All	32 672.3/5.87	182	34	9	Cyto	2.11 ± 0.25	1.33 ± 0.17	0.52 ± 0.16
32↑	Sal k 3 pollen allergen	*Salsola kali*	CL2302.Contig3_All	83 956.3/6.13	1160	51	28	Mito	0.67 ± 0.12	2.06 ± 0.30	1.31 ± 0.14
33↑	Sal k 3 pollen allergen	*Salsola kali*	CL2302.Contig3_All	83 956.3/6.13	191	20	12	Mito	NDC	2.13 ± 0.21	NDT
42↑	PREDICTED: glycine dehydrogenase [decarboxylating], mitochondrial-like (GLDC)	*Solanum lycopersicum*	Unigene6360_All	88 035/6.21	466	38	24	Mito	1.45 ± 0.28	3.27 ± 0.40	2.79 ± 0.33
Protein folding and degradation (3)											
6↓	Heat shock 70 protein	*Spinacia oleracea*	CL3846.Contig2_All	75 989.3/5.12	359	32	19	Chlo	NDT	NDT	NDT
21↓	Cytosolic heat shock 70 protein	*Spinacia oleracea*	CL2772.Contig2_All	71 295.9/5.11	848	42	22	Cyto	0.31 ± 0.06	0.39 ± 0.7	0.23 ± 0.04
24↓	Cytosolic heat shock 70 protein	*Spinacia oleracea*	CL2772.Contig2_All	71 295.9/5.11	465	47	26	Cyto	NDT	NDT	NDT

Stress and defence responses (10)											
5↑	Class V chitinase from *Nicotiana tobaccum* (NtChiV)	*Nicotiana tobaccum*	Unigene15263_All	19 339.5/4.57	181	12	3	Cyto	2.09 ± 0.36	3.14 ± 0.40	3.66 ± 0.95
15↑	Pathogenesis-related protein	*Spinacia oleracea*	Unigene23540_All	18 242.9/5.0	601	85	12	Cyto	3.59 ± 0.42	2.04 ± 0.31	1.42 ± 0.15
23↑	PREDICTED: thaumatin-like protein (TLP)	*Solanum lycopersicum*	CL3714.Contig2_All	24 862.6/5.26	284	46	8	Chlo	3.68 ± 0.46	3.47 ± 0.55	4.24 ± 0.44
25↑	Cytosolic ascorbate peroxidase (APX)	*Suaeda salsa*	Unigene12777_All	27 748/5.62	377	51	11	Cyto	3.52 ± 0.40	3.95 ± 0.46	3.75 ± 0.50
30↑	Class Ib chitinase	*Limonium bicolor*	Unigene25562_All	34 041/6.90	553	67	11	Extr	2.75 ± 0.45	2.11 ± 0.34	1.21 ± 0.27
40↑	Fe-superoxide dismutase (Fe-SOD)	*Phytolacca acinosa*	Unigene22916_All	30 624.4/7.11	351	56	12	Chlo	1.59 ± 0.17	1.49 ± 0.13	2.57 ± 0.56
41↑	Dehydroascorbate reductase (DHAR)	*Spinacia oleracea*	Unigene17662_All	30 782.6/8.47	518	60	15	Chlo	1.56 ± 0.19	0.92 ± 0.20	2.34 ± 0.26
44↑	PREDICTED: thaumatin-like protein (TLP)	*Solanum lycopersicum*	CL3714.Contig2_All	24 862.6/5.26	281	65	10	Chlo	1.74 ± 0.29	2.43 ± 0.24	1.52 ± 0.17
45↑	Probable phospholipid hydroperoxide glutathione peroxidase (PHGPX)	*Spinacia oleracea*	Unigene20325_All	19 056.5/5.58	290	63	9	Chlo	1.3 ± 0.18	1.91 ± 0.30	2.03 ± 0.21
48↑	Beta-1,3-glucanase	*Nepenthes alata*	Unigene1395_All	40 824.3/4.47	495	47	9	Chlo	0.82 ± 0.11	1.74 ± 0.17	2.16 ± 0.31
Metabolism (2)											
11↓	Ferritin-1,chloroplastic-like	*Fragaria vesca* subsp. *vesca*	Unigene19810_All	28 931.6/5.94	376	46	10	Chlo	0.52 ± 0.05	0.73 ± 0.12	0.25 ± 0.04
20↓	Pierisin	*Medicago truncatula*	CL462.Contig4_All	57 915.6/5.09	871	61	23	Cyto	NDC	0.27 ± 0.06	0.51 ± 0.10
Cell structure (2)											
16↑	Caffeoyl-CoA O-methyltransferase (CCoAMT)	*Mesembryanthemum crystallinum*	CL438.Contig1_All	28 968.8/5.23	289	46	8	Cyto	3.54 ± 0.34	2.54 ± 0.37	3.61 ± 0.37
35↑	Profilin	*Chenopodium album*	CL2478.Contig2_All	14 197.1/4.83	267	51	5	Cyto	1.42 ± 0.16	1.92 ± 0.19	2.19 ± 0.30
Unknown proteins (7)											
10↑	Unnamed protein product	*Thellungiella halophila*	Unigene7072_All	29 345/6.32	292	36	9	Chlo	1.60 ± 0.17	2.71 ± 0.31	2.89 ± 0.38
13↓	Predicted protein	*Populus trichocarpa*	Unigene25619_All	61 127.4/5.19	699	45	23	Chlo	0.34 ± 0.05	0.47 ± 0.07	0.27 ± 0.03
27↑	Conserved hypothetical protein	*Ricinus communis*	CL216.Contig3_All	82 743.9/5.80	114	36	15	Cyto	NDC	NDT	NDT
34↑	Hypothetical protein OsI_23055	*Oryza sativa indica* group	Unigene9784_All	16 807.4/4.68	241	49	7	Chlo	1.76 ± 0.20	3.38 ± 0.23	1.47 ± 0.17
2↑	Unknown								2.35 ± 0.27	1.93 ± 0.32	1.53 ± 0.18
31↑	Unknown								0.97 ± 0.17	2.05 ± 0.30	1.28 ± 0.23
46↑	Unknown								1.46 ± 0.15	2.21 ± 0.19	1.89 ± 0.25

[a]Assigned spot number as indicated in Fig. 5. Arrows indicate up- (↑) and down- (↓) regulation of the proteins.
[b]The name and functional categories of the proteins identified by matrix-assisted laser desorption ionization tandem time-of-flight mass spectrometry (MALDI-TOF/TOF MS/MS). The MALDI-TOF/TOF MS/MS results are presented, if available.
[c]The plant species that matched the peptides.
[d]Database accession numbers from the EST database of *Halogeton glomeratus*.
[e]Theoretical mass (kDa) and pI of identified proteins.
[f]The Mascot score obtained after searching against the EST database of *H. glomeratus*.
[g]The amino acid sequence coverage for the identified proteins.
[h]The number of unique peptides identified for each protein.
[i]The cellular location of identified proteins as predicted by TargetP (http://www.cbs.dtu.dk/services/TargetP) and/or PSORT (http://psort.hgc.jp/). Chlo, chloroplast; Mito, mitochondria; Cyto, cytoplasm; Nucl, nucleus; Extra, extracellular.
[j]Fold change is expressed as the ratio of the vol% between stresses (200 mM NaCl for 24 h, 72 h and 7 d) and control (0 mM NaCl). Values are presented as means ± SE of triplicates (n = 3). For some spots, which completely are absent in either stressed or control samples, the abbreviation NDC (not detected in control) or NDT (not detected in treatment) was used.

lower priority database. The alignments end when all alignments were finished. Proteins with highest rank in Blast results were taken to decide the coding region sequences (CDS) of unigenes, and then CDS were translated into amino sequences with the standard codon table. So both the nucleotide sequences (5′→3′) and the amino sequences of the unigene coding region were acquired. More detailed results of nucleotide sequence and coding region sequences (CDS) of unigenes are shown in Supporting Information Appendix S1.

Protein classification and hierarchical cluster analysis

The functional information for the identified proteins was extracted from Blast searches against the NCBI (http://www.ncbi.nlm.nih.gov/protein) and UniProt (http://www.uniprot.org) databases. These findings were combined with reports from the literature. Proteins were classified into different categories based upon their biochemical functions, according to the convention used by Jiang *et al*. (2007). The sub-cellular location information of each protein was obtained using the Target P (http://www.cbs.dtu.dk/services/TargetP/) or PSORT (http://psort.hgc.jp/) software prediction programs. A self-organizing tree algorithm of hierarchical clustering of protein relative abundance profiles was performed on the log-transformed fold change values of protein spots using Cluster software (version 3.0; http://rana.lbl.gov/EisenSoftware).

Statistical analysis

We used the one-way analysis of variance and Duncan's multiple range test to detect significant differences among means of the plant treatment groups using SPSS 16.0 statistical software (SPSS Inc., Chicago, IL, USA). A P-value <0.05 was considered statistically significant. All of the results are represented as mean ± standard error of the mean (SEM) of at least three replications.

RESULTS

Effect of salt concentration on seedling growth of *H. glomeratus*

Plant grew well with different concentrations of NaCl. Compared with control, higher NaCl concentrations (300–500 mM) significantly inhibited seedling growth. The growth of *H. glomeratus* slightly increased with increasing salt concentration, and optimal growth occurred under 100 mM NaCl conditions. The plant FW, DW and TWC reached maximum values under 100 mM NaCl. Salinity higher than 100 mM significantly decreased plant FW and DW, but high saline conditions did not affect TWC (Fig. 1a–c). Compared with the control seedlings, the FW and DW of seedlings treated with 500 mM NaCl decreased by 68 and 64%, respectively. However, at 500 mM NaCl, the seedlings did not experience any seedling death.

Anatomical structure analysis of *H. glomeratus*

We did not observe any anatomical differences among the seedlings exposed to different salinity conditions. By examining cross sections of tissues, we found that successive cambia phenomenon was present in the roots and stems, and the leaves displayed succulence (Fig. 2). In the succulent leaves, the main vascular bundle in the centre was surrounded by well-developed water-storage tissue and small peripheral bundles contacted the circle of thick-walled bundle sheath cells. Beneath the two layers of epidermal cells, the palisade tissue consisted of elongated and densely arranged cells. As far as we know, this is the most comprehensive observation of the anatomic structure of *H. glomeratus*.

Ion contents, salt crystals and stomata changes in leaves under NaCl stress

Sodium concentration in leaves of plants treated with 100, 200, 300 and 400 mM NaCl for 21 d increased by 3.44-, 4.58-, 5.27- and 6.79-fold, respectively, compared with controls. The Na concentration was highest in leaves of plants treated with 500 mM NaCl and reached 170.32 mg g^{-1} DW. Conversely, the potassium concentration in leaves decreased with increasing salt concentration. However, the potassium concentration plateaued and no further decreases were evident for NaCl concentrations greater than 200 mM (Fig. 1d). The K^+/Na^+ ratio decreased with increasing NaCl concentration (Fig. 1e).

The SEM studies revealed that the amount of salt crystals deposited in leaf water-storage tissues increased with increasing NaCl concentrations (Fig. 3). The micromorphology of stomata structure exhibited obvious changes under different salt concentrations. Under the aggravation of salt stress, especially under higher salt concentrations, convex structures developed outside the stomatal guard cells (Fig. 4).

Identification and classification of differentially abundant proteins after NaCl treatments

To investigate the changes in the proteome profiles of the leaves of *H. glomeratus* seedlings subjected to NaCl stress, we determined the abundance patterns of salt-responsive proteins using a 2-DE gel. On the gel (pH 3–10), we observed that most of the protein spots were distributed in the acidic area. Therefore, we applied narrow pH-range strips (pH 4–7) and detected approximately 1000 CBB-stained protein spots on the gels (Fig. 5 and Supporting Information Fig. S1). The global pattern of protein relative abundance remained largely unaltered. Statistical analysis of images revealed that 49 reproducibly detected spots exhibited more than twofold difference with $P < 0.05$. Most of these proteins increased in abundance, but some of the protein spots were completely absent in either treated or control samples. These protein spots were subjected to in-gel digestion and submitted for protein identification (Fig. 5 and Supporting Information Fig. S1 and Table S1). A total of 36 protein spots exhibited increased abundance and 13 spots exhibited decreased

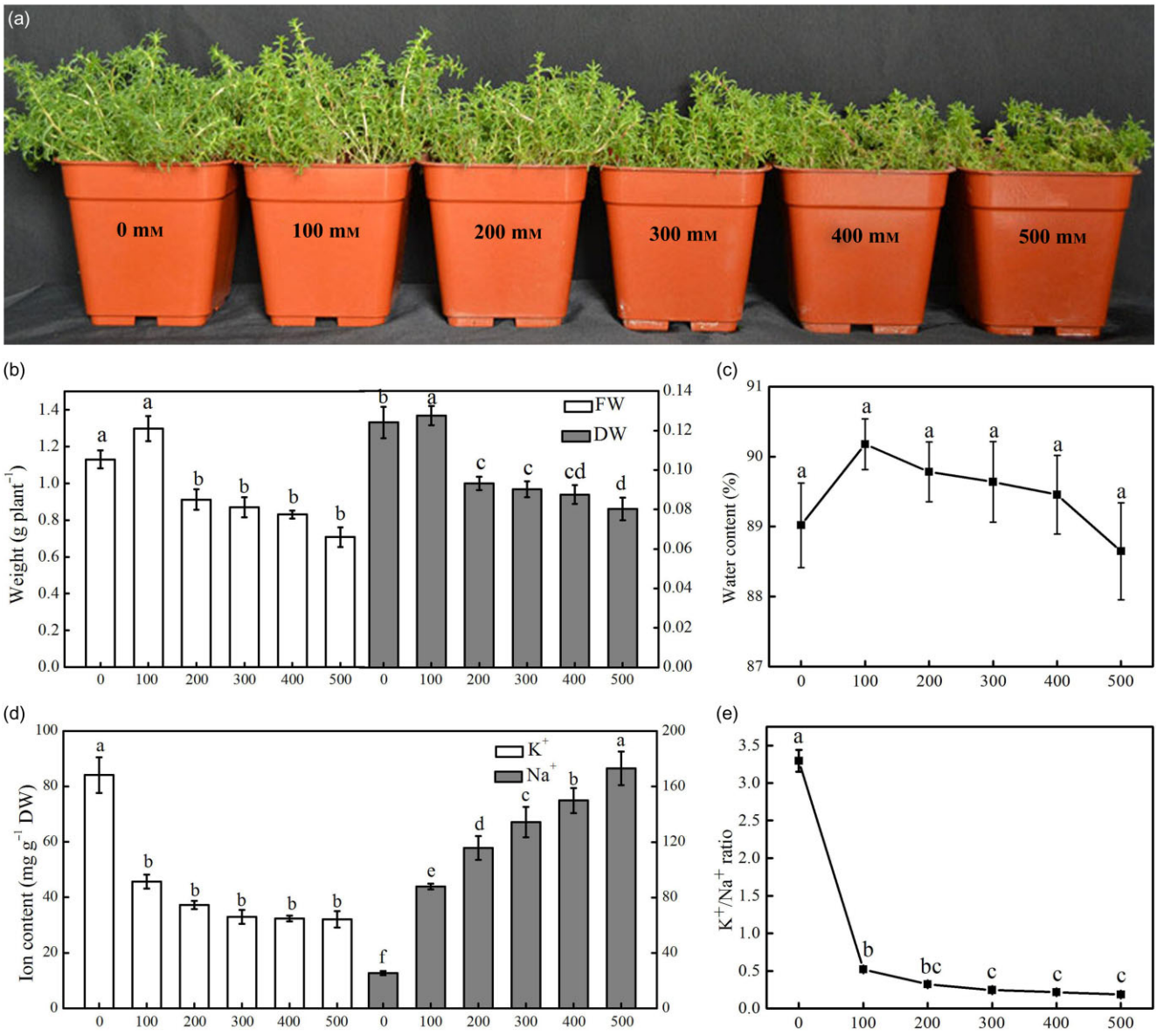

Figure 1. The effect of salinity on the growth, water content and ion content of *Halogeton glomeratus*. The plants were irrigated with half-strength Hoagland's solution with different concentrations of NaCl for 21 d (a). The effects of increasing NaCl salinity on fresh weight (FW) and dry weight (DW) (b), water content (c), K^+ and Na^+ contents (d), and the K^+/Na^+ ratio (e) in the leaves of the treated plants. The values are presented as means ± standard error (SE); $n = 5$ for all groups. The bars represent the SE. Bars with the same letter are not significantly different, denoted by $P < 0.05$ according to Duncan's multiple range test.

abundance. Of the 49 protein spots analysed via MALDI TOF/TOF MS/MS, 46 were confidently assigned to protein sequences in the EST database of *H. glomeratus*, whereas 3 spots did not retrieve a significant match when the spectra were searched against the database (Table 1 and Supporting Information Table S2). In this study, heat shock proteins (spots 6, 21 and 24), RuBisCO small subunit 1 (spot 3 and 29), thaumatin-like protein (spot 23 and 44), transketolase (spot 28 and 38) and sal k 3 pollen allergen (spots 32 and 33) were identified in more than one spot on the same gel. This phenomenon may have resulted from the presence of different protein isoforms, post-translational modification or degradation (Gao *et al*. 2009).

The proteins were grouped into nine categories based upon their biochemical functions, including photosynthesis, carbohydrate and energy metabolism, translation and transcription, amino acid metabolism, protein folding and degradation, stress and defence response, metabolism, cell structure and unknown functions (Table 1). Among these categories, photosynthesis (22.5%), stress and defence responses (20.4%), unknown functions (14.3%), carbohydrate and energy metabolism (10.2%), translation and transcription (10.2%), and amino acid metabolism (8.2%) were the most commonly represented functions.

As shown in Fig. 6, we performed a hierarchical clustering analysis of 42 proteins of known function. The analysis

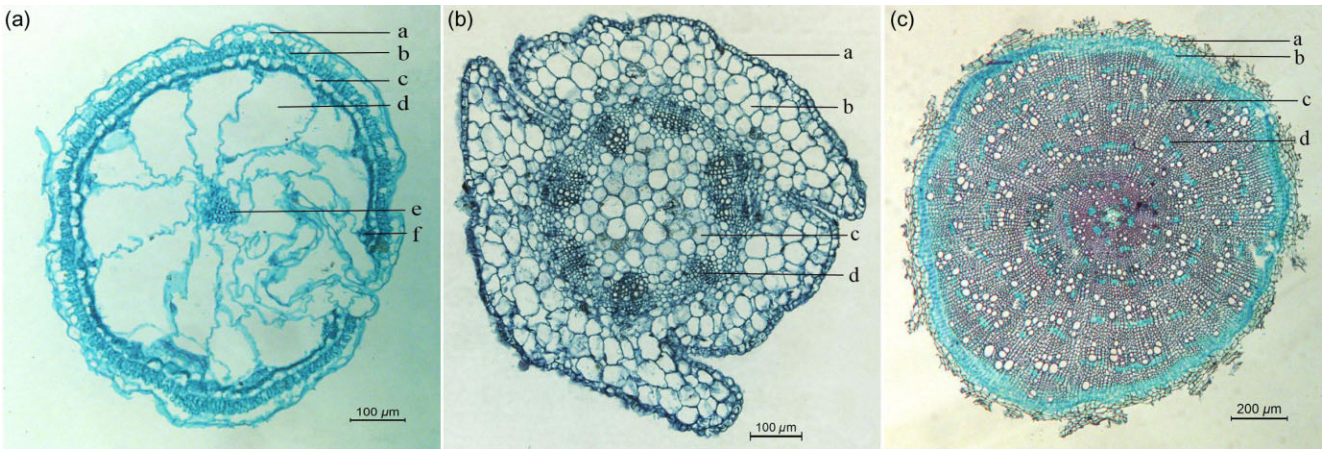

Figure 2. Transverse sections of leaf, stem and root of *Halogeton glomeratus* seedlings. (a) Leaf, exhibiting epidermal cells (a), palisade tissue (b), lignified cells (c), water-storage tissue (d), vascular bundle (e) and small peripheral bundles (f). (b) Stem, showing epidermal cells (a), cortex (b), hollow pith (c) and collateral vascular bundle (d). (c) Root, exhibiting cortex (a), secondary phloem (b), xylem (c) and large parenchyma cells (d).

formed two main clusters. Cluster I included 12 protein spots that mainly exhibited decreased relative abundance under salt treatment; cluster II included 30 protein spots that mainly exhibited increased relative abundance under salt treatment. The number of salt-induced proteins was significantly higher than the number of proteins that were down-regulated under salt conditions. In cluster I, most of these protein spots were related to photosynthesis (spots 17, 28, 37 and 38), and translation and transcription (spots 18 and 39). Cluster II included proteins involved in photosynthesis, carbohydrate and energy metabolism, translation and transcription, amino acid metabolism, and stress and defence response. Specifically, the abundance of proteins related to stress and defence (spots 5, 23, 25, 40, 44 and 45), carbohydrate and energy metabolism (spots 4 and 8), and cell structure (spots 16 and 35) was substantially increased under salt conditions. This cluster also contained three salt-inducible proteins, including two photosynthesis-related proteins (spots 9 and 14) and one amino acid metabolism-related proteins (spot 33). Furthermore, to generate a board survey of leaf proteins with altered abundance during various stage of salt stress, a Venn diagram was conducted to show the dynamics of the number of differentially abundant proteins spots under different NaCl-treated time points. As shown in Fig. 7, of the 49 protein spots, 25 spots were up-regulated and 10 spots were down-regulated at all three stages during salt stress. Fourteen spots were either up-regulated or down-regulated at least one time point after salt treatment. Together, these results suggest changes in the biological processes of adaptation to salt stress in seedlings of *H. glomeratus*.

DISCUSSION

Growth of *H. glomeratus* under different salt conditions

Halophytes are specialized organisms with well-adapted morphological, anatomical and physiological characteristics that enable the plants to survive in an environment that includes soil with a high salt concentration (Flowers & Colmer 2008). The present study showed that the growth of *H. glomeratus* increased slightly when plants were treated with 100 mM NaCl, and the growth gradually declined when NaCl concentrations were higher than 200 mM (Fig. 1a). Therefore, we considered 100 mM NaCl to be the optimal level of salinity for the growth of this plant. Salt-induced growth reduction under conditions of high salinity and growth stimulation under conditions of moderate salinity have been reported for many halophytes, such as *S. europaea* (Fan *et al*. 2011), *Atriplex halimus* L. (Hassine *et al*. 2008) and *Suaeda salsa* (Wu *et al*. 2012). Compared with the controls in this study, the DW and FW of the plants decreased significantly when the NaCl concentration was greater than 200 mM. The DW and FW decreased by 37.4 and 13.8%, respectively, with 500 mM NaCl treatment. However, no significant changes were observed in the water content of the leaves at low or high salinities (Fig. 1c). No obvious symptoms of ion deficiency or toxicity were observed in plants treated with 500 mM NaCl. These results indicate that *H. glomeratus* has a robust ability to tolerate salt stress. The roles of salt tolerance are probably to maintain TWC, increase succulence and maintain a positive water balance in response to salinity stress. This agrees with previous research in other halophytes (Eisa *et al*. 2012).

Osmotic adjustment and intracellular ion balance under salt stress

Osmotic adjustment is associated with a substantial accumulation of sodium and chloride ions in all plant organs (Flowers 2004). Tissue tolerance of salinity requires compartmentalization of sodium and chloride ions at the cellular and intracellular levels to avoid toxic concentrations in the cytoplasm, especially in mesophyll cells in leaves (Munns & Tester 2008). Our research showed that the sodium content in leaves increased dramatically with

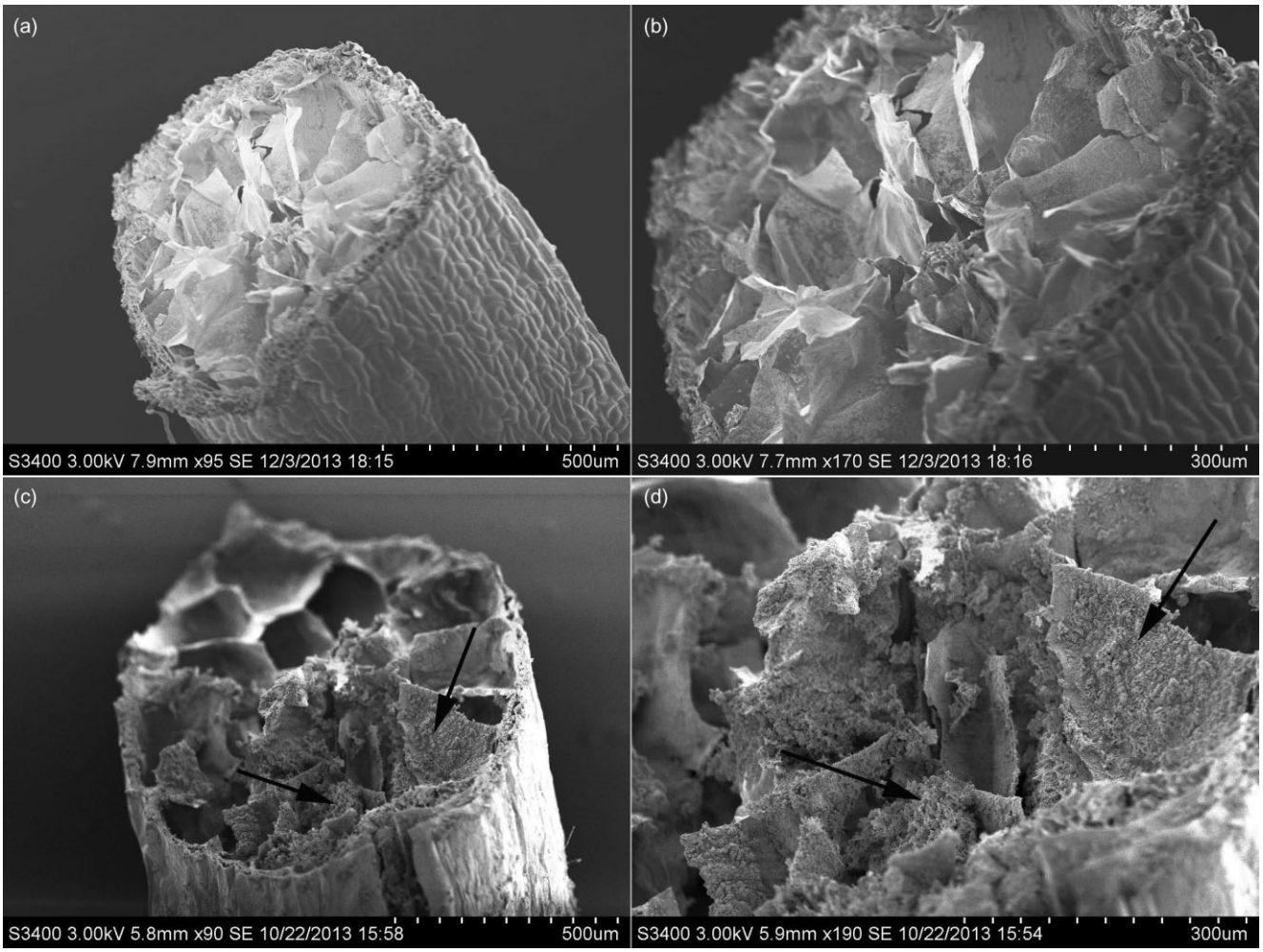

Figure 3. Micrograph of salt crystals in the water-storage tissue of a *Halogeton glomeratus* leaf. The plants were irrigated with half-strength Hoagland's solution with no NaCl (a, b) and 400 mM NaCl (c, d) for 21 d. (b, d) Partial enlargement of *H. glomeratus* leaves. Arrows indicate abundant salt crystal deposits in the water-storage tissue in plants treated with NaCl.

increasing salinity, whereas the potassium content in leaves decreased when salt concentrations increased to 200 mM NaCl. The potassium content plateaued and did not exhibit further significant changes when salt concentrations were higher than 200 mM after 21 d of salt stress (Fig. 1d). Potassium is an essential ion for various physiological processes; it is involved in protein synthesis and enzyme activation and it decreases transpirational water loss (Yu *et al*. 2011; Meychik

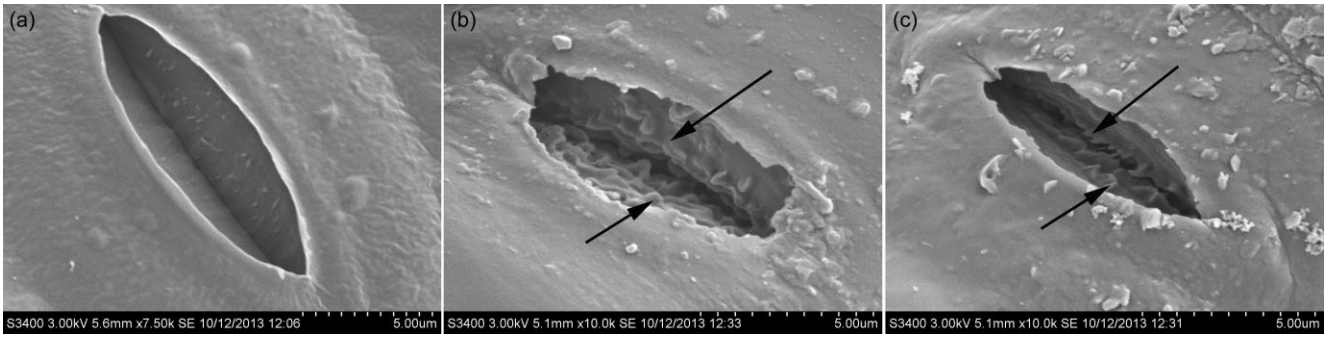

Figure 4. Micrograph of stomata on the abaxial surface of *Halogeton glomeratus* leaves. The plants were treated with half-strength Hoagland's solution with no NaCl (a), 200 mM NaCl (b) and 400 mM NaCl (c) for 21 d. Arrows indicate convex structures that formed outside the guard cells in salt-treated leaves.

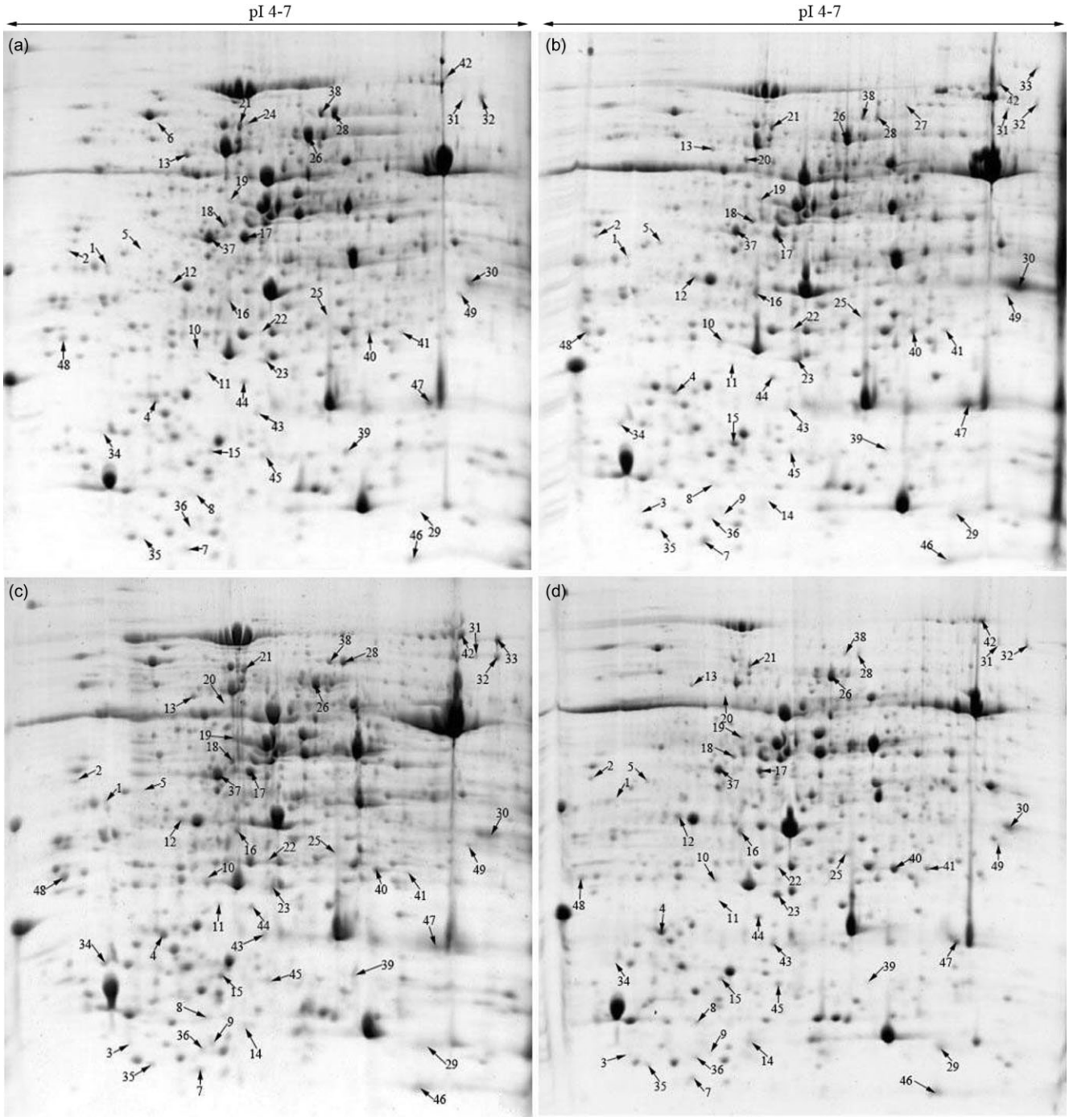

Figure 5. Representative two-dimensional gel electrophoresis (2-DE) gels of proteins extracted from leaves of *Halogeton glomeratus* treated with 200 mM NaCl for 0 h (a), 24 h (b), 72 h (c) and 7 d (d). Arrows indicate the 49 protein spots that were positively identified.

et al. 2013). Seedlings must re-establish intracellular ion homeostasis through osmotic adjustment in leaves under salt stress (Meychik *et al*. 2013). We observed the deposition of salt crystals in the water-storage tissues in leaves under salt stress. The salt-inducible Na^+/H^+ antiporter plays an important role in the accumulation of sodium ions by transporting them across the tonoplast into vacuoles (Wang *et al*. 2001). This process is associated with an increase in the activity of the Na^+/H^+ antiporter (Qiu *et al*. 2007). On the contrary, we did observe slight changes in the TWC of leaves under salt stress, which contributed to a reduction in the osmotic potential of plant cells. Enhanced succulence and TWC could improve the plant's salt tolerance.

In addition to adjusting the water content, the accumulation of compatible organic solutes, such as proline and betaine, is one of the most important anti-salinity

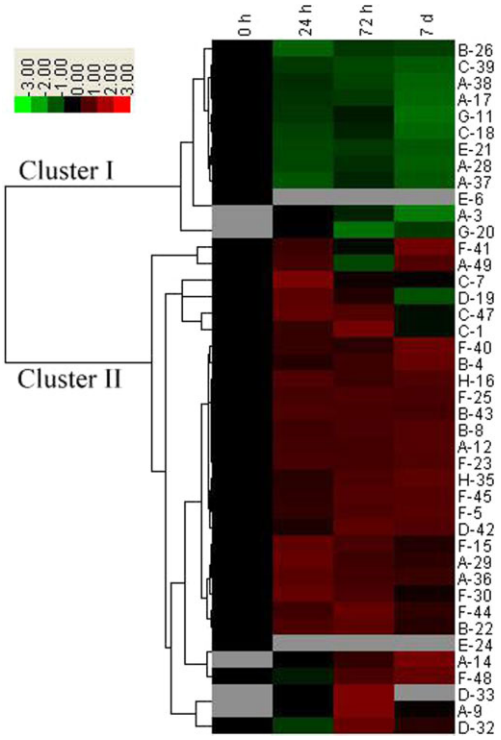

Figure 6. Hierarchical clustering analysis of the expression profiles of the 42 identified proteins. The four columns represent different NaCl treatments; columns 1, 2, 3 and 4 represent treatment for 0 h, 24 h, 72 h and 7 d, respectively, with 200 mM NaCl. The rows represent individual proteins. The protein cluster is on the left side, and the treatment cluster is on the top. The up- and down-regulated proteins are indicated in red and green, respectively. The grey boxes indicate proteins that were not detected on the 2-DE gels. The intensity of the colours increases with increasing expression differences, as shown in the legend. The protein spot numbers are listed on the right, and the letters before the spot numbers represent various functional categories of the proteins: A, photosynthesis; B, carbohydrate and energy metabolism; C, translation and transcription; D, amino acid metabolism; E, protein folding and degradation; F, stress and defence responses; G, metabolism; H, cell structure.

mechanisms used by plants to maintain a stable osmotic pressure and protect macromolecules from degradation (Guo *et al*. 2010). Our proteomics analysis revealed two proteins related to the accumulation of organic solutes. Plastid glutamine synthetase 2 (GS 2; spot 19) plays a key role in nitrogen metabolism, which is responsible of ammonium assimilation and transformation into glutamine (Gadaleta *et al*. 2011), and the increased activity of GS2 enhanced nitrogen assimilation and the activities of enzymes involved in carbon and nitrogen metabolism in transgenic tobacco grown under low nitrogen conditions (Wang *et al*. 2013b). Glycine dehydrogenase (GLDC; spot 42) is crucial for glycine betaine biosynthesis. The accumulation of proline and glycine betaine facilitates coping mechanisms in plants under salt stress by mediating osmotic adjustment (Guo *et al*. 2010). The up-regulation of GS2 and GLDC observed in this study suggests that the accumulation of compatible organic solutes in leaves may be related to salt tolerance of *H. glomeratus*.

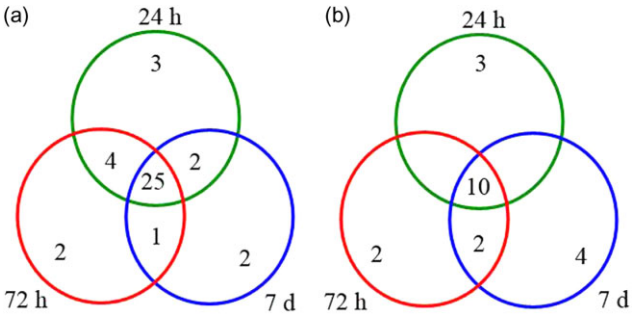

Figure 7. Venn diagram analysis of the number of up- or down-regulated protein spots in *Halogeton glomeratus* seedlings under different time course (24 h, 72 h and 7 d) of 200 mM NaCl stress. Results are presented as average of three independent experiments: (a) up-regulated protein spots and (b) down-regulated protein spots.

Photosynthesis under salt stress

Salt stress causes a growth rate reduction due to inadequate photosynthesis in plants. This phenomenon occurs because of stomatal closure and the consequent limited carbon dioxide uptake (Zhu 2001). In this study, we identified 11 protein spots involved in photosynthesis, and their abundance was significantly changed by salt treatments (Table 1). Of these, six protein spots are related to CO_2 assimilation. Ribulose bisphosphate carboxylase small chain 1, chloroplastic (RuBisCO small subunit 1; spots 3 and 29), ribulose-1,5-bisphosphatecarboxylase/oxygenase large subunit (RuBisCO LSU; spot 9), ribulose 1,5-bisphosphatecarboxylase/oxygenase small subunit (RuBisCO small subunit; spot 14 and 36) and beta carbonic anhydrase 2 (BCA2; spot 49) were up-regulated under salt treatment. Furthermore, spot 14 was a protein that was absent in the controls, but exhibited an increased abundance under salt conditions. RuBisCO is the key enzyme in the Calvin cycle and mediates photosynthetic CO_2 assimilation by catalysing the reaction of D-ribulose 1,5-bisphosphate and CO_2 to two 3-phospho-D-glycerate molecules. The up-regulation of RuBisCO activase under salinity stress has been reported previously (Yang *et al*. 2012). A key protein of photosynthetic light reaction, oxygen-evolving enhancer protein 1 (OEE1, spot 12), was also up-regulated under NaCl conditions. The enzymes related to the Calvin cycle, such as phosphoribulokinase (PRKase; spot 17), putative transketolase (TK, spots 28 and 38), sedoheptulose-1,7-bisphosphatase [SED(1,7)P2ase, spot 37] were down-regulated under salt conditions. This implies that up-regulation of CO_2 fixation and light reaction-related proteins might result in an enhanced photosynthetic CO_2 assimilation and improve the light-capturing ability of plants. This is consistent with studies in halophytes, including *S. europaea* (Wang *et al*. 2009), and wild halophytic rice (Sengupta & Majumder 2009). However, some photosynthesis-related enzymes, such as RuBisCO activase, chlorophyll *a/b* binding protein (CAB) and oxygen-evolving enhancer protein 1 (OEE 1), were decreased in *Puccinellia tenuiflora* (Yu *et al*.

2011) and *Aeluropus lagopoides* (Sobhanian *et al*. 2010). In this study, we observed no obvious changes in stomata opening or closing in different saline environments, which supports previous findings (Gaxiola *et al*. 2001; Munns & Tester 2008; Lokhande & Suprasanna 2012), but we did observe the formation of convex structures outside the guard cells under salt conditions (Fig. 4). We suspect that these structures might, to some extent, prevent water transpiration from stomata under abiotic stress. These results suggest that stomatal structure is one of the photosynthetic strategies that allow *H. glomeratus* to survive in high salinity environments. Consistent with our results, previous studies have shown that the levels of proteins related to CO_2 assimilation and light reactions of the Calvin cycle increased under salt stress. On the contrary, low intercellular CO_2 concentrations could decrease the activity of Calvin cycle enzymes, which explains the decrease in the rate of photosynthesis under salt stress (Ndimba *et al*. 2005; Jiang *et al*. 2007; Zhang *et al*. 2011). The results of our proteomic analysis indicate growth inhibition under conditions of high salinity.

Carbohydrate and energy metabolism under salt stress

Carbohydrate metabolism, including pentose phosphate pathway (PPP), glycolysis, and the TCA cycle, is rapidly adjusted under salt stress. Large amounts of ATPase are needed to provide energy for the growth and development of plants under conditions of high salinity (Wang *et al*. 2009). In this study, we identified four proteins that were enzymes related to carbohydrate metabolism and one that was involved in energy metabolism. The high abundance levels of NAD(P)H-quinone oxidoreductase subunit M (NDH-1 subunit M; spot 4), triosephosphate isomerase (TIM; spot 22) and lactoylglutathione lyase-like (spot 43) implied that the PPP and glycolysis increased under salt conditions. Increased activity of the PPP provides more glyceraldehyde-3-phosphate and glucose-6-phosphate into the glycolysis pathway, which is the central pathway for energy production in higher plants. The up-regulation of these proteins results in increased ATP production in cell, which improves plant tolerance against salt stress.

We observed the up-regulation of ATP synthase subunit beta (spot 8), which is consistent with the findings of previous proteomic studies (Sobhanian *et al*. 2010; Kosová *et al*. 2011). However, the NADP-malic enzyme (NADP-ME, spot 26) was down-regulated under salt stress. NADP-ME is related to the TCA cycle and is responsible for the decarboxylation of malate to pyruvate; NADP-ME is a source for CO_2, NADPH and pyruvate (Lai *et al*. 2002). The energy status of the cell is controlled by the activity of enzymes in the TCA cycle. For example, the activity of malate dehydrogenase decreases in NaCl-treated *Arabidopsis* roots (Jiang *et al*. 2007). The different abundance levels of these proteins imply that salt stress results in alterations to metabolic activities in order for plants to adapt to salt conditions.

Protein synthesis under salt stress

The abundance levels of five proteins related to translation and transcription changed markedly after salt treatment. The following proteins were up-regulated under saline conditions: elongation factor 1-delta (eEF-1B beta; spot 1), nuclear transport factor, putative (NTF; spot 7) and transcription factor BTF3 (spot 47). Chloroplast ribosomal protein S1 (spot 18) and eukaryotic translation initiation factor 5A2 (eIF 5A2; spot 39) were down-regulated.

Transcription-related proteins and transcription factors are responsive to salt stress and play a crucial role in salinity tolerance (Zhang *et al*. 2008; Kosmala *et al*. 2009). Up-regulated eEF-1B and BTF3 in conditions of salt stress help to maintain normal protein synthesis to improve salt tolerance. The down-regulated level of eIF 5A2 under salt stress indicates the premature senescence of plants (Pang *et al.*, 2010). Chloroplast ribosomal protein S1 (spot 18) showed an obvious decrease in abundance, which indicated that protein biosynthesis was inhibited by NaCl. Similarly, previous reports showed that ribosomal proteins were down-regulated under osmotic stress and heat stress (Askari *et al*. 2006; Alam *et al*. 2010). Together, the changes in abundance levels of these proteins suggest that protein biosynthesis is affected under conditions of high salinity. Further, these proteins play important roles in salt tolerance of *H. glomeratus*.

We observed two protein spots related to amino acid biosynthesis in leaves that were up-regulated under salt stress. Sal k 3 pollen allergen (spots 32 and 33) is a cobalamin-independent methionine synthase and catalyses the transfer of a methyl group from 5-methyltetrahydrofolate to homocysteine, which results in methionine formation (Wang *et al*. 2009). Methionine synthase is believed to be related to lignification of the cell wall. Up-regulation of these proteins was correlated with changes in the anatomical structure of leaves under salt stress, which results in increased vessel development in the leaves of *H. glomeratus*.

Proteins related to folding, transport and degradation under salt stress

The abundance of three Hsp70 proteins (spots 6, 21 and 24) decreased under salt conditions. Hsp70s are expressed in response to environmental stress conditions, such as heat, cold, drought and salinity (Askari *et al*. 2006). Here, we observed decreased levels of Hsp70 in the leaves. Hsp70s serve various overlapping roles in maintaining the integrity of other proteins and the removal of non-functional, but potentially harmful, polypeptides (Ndimba *et al*. 2005; Sengupta & Majumder 2009). Hsp70s were also reported to be involved in transporting precursor proteins through the membranes (Ndimba *et al*. 2005). The down-regulation of Hsp70s after NaCl treatment suggests a decrease in the transportation of newly synthesized peptides and low protein synthesis under high salinity conditions (Jiang *et al*. 2007).

Stress defence and other stress-responsive proteins

The reduced rate of photosynthesis and structural changes in the chloroplast should enhance the production of ROS under salt stress (Barkla *et al*. 2013). The enzymatic antioxidant system is one of the protective mechanisms employed to eliminate or reduce ROS under abiotic stress (Mittler *et al*. 2004). Enhanced antioxidant activity is suggested to be the more radical approach for increasing a plant's capacity for stress tolerance (Jithesh *et al*. 2006). The results of our proteomics analysis revealed that the abundance levels of four antioxidative enzymes increased under salt conditions to regulate the balance of ROS formation and removal and defence against oxidative stress and cell damage. Cytosolic ascorbate peroxidase (APX; spot 25), Fe-superoxide dismutase (Fe-SOD; spot 40) and probable phospholipid hydroperoxide glutathione peroxidase (PHGPX; spot 45) play crucial roles in defending against oxidative stress (Kosmala *et al*. 2009). Dehydroascorbate reductase (DHAR; spot 41) is one of the key enzymes in maintaining the regeneration of ascorbate (AsA), which is a major antioxidant that detoxifies ROS (Noctor & Foyer 1998; Yin *et al*. 2010). The increased abundance levels of four enzymes in salt stress conditions indicate that detoxifying and antioxidant enzymes have important roles in a plant's response to salinity.

In addition, five protein spots of increased abundance levels after salt treatment were identified as pathogenesis-related (PR) proteins. Class V chitinase from *Nicotiana tobaccum* (NtChiV; spot 5) and class Ib chitinase (spot 30) belong to different classes of chitinase, which have been conferred with self-defence by attacking chitin (Bishop *et al*. 2000), response to various abiotic and biotic stresses (Bishop *et al*. 2000; Chen *et al*. 2014). Thaumatin-like protein (TLP, spots 21 and 44) plays an important role in secondary cell wall development of plants. Overexpression of TLP gene enhanced resistance to diseases of plants (Munis *et al*. 2010; Koga *et al*. 2012).

Furthermore, we also observed that the up-regulation of proteins associated with profiling (spot 35), which is associated with cytoskeleton remodelling, might be involved in leaf succulence of *H. glomeratus* in response to salinity. Similar results were reported with a succulent halophyte, *S. aegyptiaca*, under salt stress (Askari *et al*. 2006). Caffeoyl-CoA O-methyltransferase (CCoAMT; spot 16) is involved in cell wall lignification and plays the essential role in the synthesis of monolignols, which are the precursors for lignin (Alam *et al*. 2010). Lignin is a biopolymer that is integrated into the reticular cellulose structure in the cell wall and is involved in the reinforcement of the plant cell wall (Sánchez-Aguayo *et al*. 2004). These results are consistent with our observations of the anatomical structures of leaves, which indicated the lignification of the cell wall under salt stress. We observed that the down-regulation of ferritin-1, chloroplastic-like (spot 11) after salt treatment, which was reported to be involved in drought-stress responses of barely (Zhang *et al*. 2014), is hypothesized to store ferrous iron in the chloroplast in a non-toxic form and to protect plants from oxidative damage induced by a wide range of stressors (Deák *et al*. 1999). The changes in abundance levels of these proteins imply that *H. glomeratus* has a system of salt tolerance mechanisms to adapt to conditions of high salinity.

CONCLUSION

To the best of our knowledge, this is the first systematic report on salt tolerance mechanisms in *H. glomeratus* based upon physiological, anatomical and proteomic analyses. The present results demonstrate that *H. glomeratus* has a robust resistant to salinity, and it showed optimal growth under 100 mM NaCl condition. After salt treatment, *H. glomeratus* accumulated large amounts of sodium in water-storage tissue in leaves, maintained the water content of tissues and the succulence of leaves, and formed convex structures outside the stomatal guard cells in response to salt stress.

Quantitative analysis of more than 1000 protein spots on 2-DE gels revealed significant variations in 49 protein spots from the leaves of salt-treated plants. Of these, 46 protein spots were positively identified by MALDI-TOF/TOF MS/MS and similarity searches across EST database of *H. glomeratus*. These proteins were classified into nine functional groups involved in photosynthesis, carbohydrate and energy metabolism, protein folding and degradation, and stress and defence responses, etc. These results suggest that photosynthesis, energy production, ion homeostasis and ROS scavenging-associated enzymes play important roles in the salt tolerance of plant. Hierarchical clustering results revealed that these proteins are involved in a dynamic network that promotes salt tolerance of *H. glomeratus*. These processes work cooperatively to achieve homeostasis under conditions of salt stress. The identification of salt-responsive proteins in *H. glomeratus* may provide new insights into the molecular mechanisms that underlie salt tolerance. Future work should integrate transcriptomic, proteomic and metabolomic approaches to define salt tolerance mechanisms of plant response and acclimation to salt stress and to clarify potential candidate salt-tolerant genes in *H. glomeratus*.

ACKNOWLEDGMENTS

This work was supported by the National Natural Science Foundation of China (No.31171558) and China Agriculture Research System (CARS-05).

REFERENCES

Alam I., Sharmin S.A., Kim K., Yang J.K., Choi M.S. & Lee B. (2010) Proteome analysis of soybean roots subjected to short-term drought stress. *Plant and Soil* **333,** 491–505.

Aoki A., Kanegami A., Mihara M., Kojima T., Shiraiwa M. & Takahara H. (2005) Molecular cloning and characterization of a novel soybean gene encoding a leucine-zipper-like protein induced to salt stress. *Gene* **356,** 135–145.

Askari H., Edqvist J., Hajheidari M., Kafi M. & Salekdeh G.H. (2006) Effects of salinity levels on proteome of *Suaeda aegyptiaca* leaves. *Proteomics* **6,** 2542–2554.

Baird W.V. & Blackwell W.H. (1980) Secondary growth in the axis of *Halogeton glomeratus* (Bieb.) Meyer (Chenopodiaceae). *Botanical Gazette* **141,** 269–276.

Barkla B.J., Castellanos Cervantes T., Diaz de León J.L., Matros A., Mock H., Perez Alfocea F., . . . Zörb C. (2013) Elucidation of salt stress defense and tolerance mechanisms of crop plants using proteomics – current achievements and perspectives. *Proteomics* **13,** 1885–1900.

Bartels D. & Dinakar C. (2013) Balancing salinity stress responses in halophytes and non-halophytes: a comparison between *Thellungiella* and *Arabidopsis thaliana*. *Functional Plant Biology* **40,** 819–831.

Bishop J.G., Dean A.M. & Mitchell-Olds T. (2000) Rapid evolution in plant chitinases: molecular targets of selection in plant-pathogen coevolution. *Proceedings of the National Academy of Sciences of the United States of America* **97,** 5322–5327.

Carpentier S.C., Panis B., Vertommen A., Swennen R., Sergeant K., Renaut J., . . . Devreese B. (2008) Proteome analysis of non-model plants: a challenging but powerful approach. *Mass Spectrometry Reviews* **27,** 354–377.

Champagne A. & Boutry M. (2013) Proteomics of nonmodel plant species. *Proteomics* **13,** 663–673.

Chen P.J., Senthilkumar R., Jane W.N., He Y., Tian Z. & Yeh K.W. (2014) Transplastomic *Nicotiana benthamiana* plants expressing multiple defence genes encoding protease inhibitors and chitinase display broad-spectrum resistance against insects, pathogens and abiotic stresses. *Plant Biotechnology Journal* **12,** 503–515.

Dayton W.A. (1951) Historical sketch of barilla. *Journal of Range Management Archives* **4,** 375–381.

Deák M., Horváth G.V., Davletova S., Török K., Sass L., Vass I., . . . Dudits D. (1999) Plants ectopically expressing the iron binding protein, ferritin, are tolerant to oxidative damage and pathogens. *Nature Biotechnology* **17,** 192–196.

Debez A., Braun H., Pich A., Taamalli W., Koyro H., Abdelly C. & Huchzermeyer B. (2012) Proteomic and physiological responses of the halophyte *Cakile maritima* to moderate salinity at the germinative and vegetative stages. *Journal of Proteomics* **75,** 5667–5694.

Duda J.J., Freeman D.C., Emlen J.M., Belnap J., Kitchen S.G., Zak J.C., . . . Montante J. (2003) Differences in native soil ecology associated with invasion of the exotic annual chenopod, *Halogeton glomeratus*. *Biology and Fertility of Soils* **38,** 72–77.

Dye W.B. (1956) *Chemical studies on* Halogeton glomeratus. *Weeds* **4,** 55–60.

Eisa S., Hussin S., Geissler N. & Koyro H.W. (2012) Effect of NaCl salinity on water relations, photosynthesis and chemical composition of quinoa (*Chenopodium quinoa* Willd.) as a potential cash crop halophyte. *Australian Journal of Crop Science* **6,** 357–368.

Fan P., Feng J., Jiang P., Chen X., Bao H., Nie L., . . . Li Y. (2011) Coordination of carbon fixation and nitrogen metabolism in *Salicornia europaea* under salinity: comparative proteomic analysis on chloroplast proteins. *Proteomics* **11,** 4346–4367.

Flowers T.J. (2004) Improving crop salt tolerance. *Journal of Experimental Botany* **55,** 307–319.

Flowers T.J. & Colmer T.D. (2008) Salinity tolerance in halophytes. *New Phytologist* **179,** 945–963.

Gadaleta A., Nigro D., Giancaspro A. & Blanco A. (2011) The glutamine synthetase (*GS2*) genes in relation to grain protein content of durum wheat. *Functional & Integrative Genomics* **11,** 665–670.

Gao F., Gao Q., Duan X., Yue G., Yang A. & Zhang J. (2006) Cloning of an H^+-PPase gene from *Thellungiella halophila* and its heterologous expression to improve tobacco salt tolerance. *Journal of Experimental Botany* **57,** 3259–3270.

Gao F., Zhou Y., Zhu W., Li X., Fan L. & Zhang G. (2009) Proteomic analysis of cold stress-responsive proteins in *Thellungiella* rosette leaves. *Planta* **230,** 1033–1046.

Gaxiola R.A., Li J., Undurraga S., Dang L.M., Allen G.J., Alper S.L. & Fink G.R. (2001) Drought-and salt-tolerant plants result from overexpression of the AVP1 H^+-pump. *Proceedings of the National Academy of Sciences of the United States of America* **98,** 11444–11449.

Guan B., Hu Y., Zeng Y., Wang Y. & Zhang F. (2011) Molecular characterization and functional analysis of a vacuolar Na^+/H^+ antiporter gene (*HcNHX1*) from *Halostachys caspica*. *Molecular Biology Reports* **38,** 1889–1899.

Guo L.Q., Shi D.C. & Wang D.L. (2010) The key physiological response to alkali stress by the alkali-resistant halophyte *Puccinellia tenuiflora* is the accumulation of large quantities of organic acids and into the rhyzosphere. *Journal of Agronomy and Crop Science* **196,** 123–135.

Guo S., Yin H., Zhang X., Zhao F., Li P., Chen S., . . . Zhang H. (2006) Molecular cloning and characterization of a vacuolar H^+-pyrophosphatase gene, *SsVP*, from the halophyte *Suaeda salsa* and its overexpression increases salt and drought tolerance of *Arabidopsis*. *Plant Molecular Biology* **60,** 41–50.

Habermann B., Oegema J., Sunyaev S. & Shevchenko A. (2004) The power and the limitations of cross-species protein identification by mass spectrometry-driven sequence similarity searches. *Molecular & Cellular Proteomics* **3,** 238–249.

Hassine A.B., Ghanem M.E., Bouzid S. & Lutts S. (2008) An inland and a coastal population of the Mediterranean xero-halophyte species *Atriplex halimus* L. differ in their ability to accumulate proline and glycinebetaine in response to salinity and water stress. *Journal of Experimental Botany* **59,** 1315–1326.

Hossain Z., Nouri M. & Komatsu S. (2011) Plant cell organelle proteomics in response to abiotic stress. *Journal of Proteome Research* **11,** 37–48.

James L.F. & Butcher J.E. (1972) Halogeton poisoning of sheep: effect of high level oxalate intake. *Journal of Animal Science* **35,** 1233–1238.

Jiang Y., Yang B., Harris N.S. & Deyholos M.K. (2007) Comparative proteomic analysis of NaCl stress-responsive proteins in *Arabidopsis* roots. *Journal of Experimental Botany* **58,** 3591–3607.

Jithesh M.N., Prashanth S.R., Sivaprakash K.R. & Parida A.K. (2006) Antioxidative response mechanisms in halophytes: their role in stress defence. *Journal of Genetics* **85,** 237–254.

Khan M.A., Gul B. & Weber D.J. (2001) Seed germination characteristics of *Halogeton glomeratus*. *Canadian Journal of Botany* **79,** 1189–1194.

Koga H., Dohi K., Nishiuchi T., Kato T., Takahara H., Mori M. & Komatsu S. (2012) Proteomic analysis of susceptible rice plants expressing the whole plant-specific resistance against *Magnaporthe oryzae*: involvement of a thaumatin-like protein. *Physiological and Molecular Plant Pathology* **77,** 60–66.

Kosmala A., Bocian A., Rapacz M., Jurczyk B. & Zwierzykowski Z. (2009) Identification of leaf proteins differentially accumulated during cold acclimation between *Festuca pratensis* plants with distinct levels of frost tolerance. *Journal of Experimental Botany* **60,** 3595–3609.

Kosová K., Vítámvás P., Prášil I.T. & Renaut J. (2011) Plant proteome changes under abiotic stress – contribution of proteomics studies to understanding plant stress response. *Journal of Proteomics* **74,** 1301–1322.

Lai L.B., Tausta S.L. & Nelson T.M. (2002) Differential regulation of transcripts encoding cytosolic NADP-malic enzyme in C_3 and C_4 *Flaveria* species. *Plant Physiology* **128,** 140–149.

Li W., Zhang C., Lu Q., Wen X. & Lu C. (2011) The combined effect of salt stress and heat shock on proteome profiling in *Suaeda salsa*. *Journal of Plant Physiology* **168,** 1743–1752.

Lokhande V.H. & Suprasanna P. (2012) Prospects of halophytes in understanding and managing abiotic stress tolerance. In *Environmental adaptations and stress tolerance of plants in the era of climate change* (eds Ahmad P. & Prasad M.N.V.), pp. 29–56. Springer, New York.

Meychik N.R., Nikolaeva Y.I. & Yermakov I.P. (2013) Physiological response of halophyte (*Suaeda altissima* (L.) Pall.) and glycophyte (*Spinacia oleracea* L.) to salinity. *American Journal of Plant Sciences* **4,** 427–435.

Mittler R., Vanderauwera S., Gollery M. & Van Breusegem F. (2004) Reactive oxygen gene network of plants. *Trends in Plant Science* **9,** 490–498.

Munis M., Tu L., Deng F., Tan J., Xu L., Xu S., . . . Zhang X. (2010) A thaumatin-like protein gene involved in cotton fiber secondary cell wall development enhances resistance against *Verticillium dahliae* and other stresses in transgenic tobacco. *Biochemical and Biophysical Research Communications* **393,** 38–44.

Munns R. & Tester M. (2008) Mechanisms of salinity tolerance. *Annual Review of Plant Biology* **59,** 651–681.

Ndimba B.K., Chivasa S., Simon W.J. & Slabas A.R. (2005) Identification of *Arabidopsis* salt and osmotic stress responsive proteins using two-dimensional difference gel electrophoresis and mass spectrometry. *Proteomics* **5,** 4185–4196.

Noctor G. & Foyer C.H. (1998) Ascorbate and glutathione: keeping active oxygen under control. *Annual Review of Plant Biology* **49,** 249–279.

Ohta M., Hayashi Y., Nakashima A., Hamada A., Tanaka A., Nakamura T. & Hayakawa T. (2002) Introduction of a Na^+/H^+ antiporter gene from *Atriplex gmelini* confers salt tolerance to rice. *FEBS Letters* **532,** 279–282.

Pang, Q., Chen, S., Dai, S., Chen, Y., Wang, Y. & Yan, X. (2010) Comparative proteomics of salt tolerance in *Arabidopsis thaliana* and *Thellungiella halophila*. *Journal of proteome research* **9,** 2584–2599.

Parker R., Flowers T.J., Moore A.L. & Harpham N.V. (2006) An accurate and reproducible method for proteome profiling of the effects of salt stress in the rice leaf lamina. *Journal of Experimental Botany* **57,** 1109–1118.

Peterson G.L. (1977) A simplification of the protein assay method of Lowry *et al*. which is more generally applicable. *Analytical Biochemistry* **83,** 346–356.

Qiu N., Chen M., Guo J., Bao H., Ma X. & Wang B. (2007) Coordinate up-regulation of V-H^+-ATPase and vacuolar Na^+/H^+ antiporter as a response to NaCl treatment in a C3 halophyte *Suaeda salsa*. *Plant Science* **172,** 1218–1225.

Renard B.Y., Xu B., Kirchner M., Zickmann F., Winter D., Korten S., . . . Steen H. (2012) Overcoming species boundaries in peptide identification with Bayesian information criterion-driven error-tolerant peptide search (BICEPS). *Molecular & Cellular Proteomics* **11,** M111–M14167.

Sánchez-Aguayo I., Rodríguez-Galán J.M., García R., Torreblanca J. & Pardo J.M. (2004) Salt stress enhances xylem development and expression of *S*-adenosyl-L-methionine synthase in lignifying tissues of tomato plants. *Planta* **220,** 278–285.

Saad R.B., Zouari N., Ramdhan W.B., Azaza J., Meynard D., Guiderdoni E. & Hassairi A. (2010) Improved drought and salt stress tolerance in transgenic tobacco overexpressing a novel A20/AN1 zinc-finger '*AlSAP*' gene isolated from the halophyte grass *Aeluropus littoralis*. *Plant Molecular Biology* **72,** 171–190.

Schuerger A.C., Brown C.S. & Stryjewski E.C. (1997) Anatomical features of pepper plants (*Capsicum annuum* L.) grown under red light-emitting diodes supplemented with blue or far-red light. *Annals of Botany* **79,** 273–282.

Sengupta S. & Majumder A.L. (2009) Insight into the salt tolerance factors of a wild halophytic rice, *Porteresia coarctata*: a physiological and proteomic approach. *Planta* **229,** 911–929.

Sheffield J., Taylor N., Fauquet C. & Chen S. (2006) The cassava (*Manihot esculenta* Crantz) root proteome: protein identification and differential expression. *Proteomics* **6,** 1588–1598.

Sinha R. & Chattopadhyay S. (2011) Changes in the leaf proteome profile of *Mentha arvensis* in response to *Alternaria alternata* infection. *Journal of Proteomics* **74,** 327–336.

Sobhanian H., Motamed N., Jazii F.R., Nakamura T. & Komatsu S. (2010) Salt stress induced differential proteome and metabolome response in the shoots of *Aeluropus lagopoides* (Poaceae), a halophyte C_4 plant. *Journal of Proteome Research* **9,** 2882–2897.

Tada Y. & Kashimura T. (2009) Proteomic analysis of salt-responsive proteins in the mangrove plant, *Bruguiera gymnorhiza*. *Plant & Cell Physiology* **50,** 439–446.

Taji T., Seki M., Satou M., Sakurai T., Kobayashi M., Ishiyama K., . . . Shinozaki K. (2004) Comparative genomics in salt tolerance between Arabidopsis and Arabidopsis-related halophyte salt cress using Arabidopsis microarray. *Plant Physiology* **135,** 1697–1709.

Tuteja N. (2007) Mechanisms of high salinity tolerance in plants. *Methods in Enzymology* **428,** 419–438.

Wang B., Lüttge U. & Ratajczak R. (2001) Effects of salt treatment and osmotic stress on V-ATPase and V-PPase in leaves of the halophyte *Suaeda salsa*. *Journal of Experimental Botany* **52,** 2355–2365.

Wang X., Fan P., Song H., Chen X., Li X. & Li Y. (2009) Comparative proteomic analysis of differentially expressed proteins in shoots of *Salicornia europaea* under different salinity. *Journal of Proteome Research* **8,** 3331–3345.

Wang X., Chang L., Wang B., Wang D., Li P., Wang L., . . . Guo A. (2013a) Comparative proteomics of *Thellungiella halophila* leaves under different salinity revealed chloroplast starch and soluble sugar accumulation played important roles in halophyte salt tolerance. *Molecular & Cellular Proteomics* **12,** 2174–2195.

Wang Y., Fu B., Pan L., Chen L., Fu X. & Li K. (2013b) Overexpression of *Arabidopsis* Dof1, GS1 and GS2 enhanced nitrogen assimilation in transgenic tobacco grown under low-nitrogen conditions. *Plant Molecular Biology Reporter* **31,** 886–900.

Wu C., Gao X., Kong X., Zhao Y. & Zhang H. (2009) Molecular cloning and functional analysis of a Na^+/H^+ antiporter gene *ThNHX1* from a halophytic plant *Thellungiella halophila*. *Plant Molecular Biology Reporter* **27,** 1–12.

Wu H., Liu X., You L., Zhang L., Zhou D., Feng J., . . . Yu J. (2012) Effects of salinity on metabolic profiles, gene expressions, and antioxidant enzymes in halophyte *Suaeda salsa*. *Journal of Plant Growth Regulation* **31,** 332–341.

Yadav N.S., Shukla P.S., Jha A., Agarwal P.K. & Jha B. (2012) The *SbSOS1* gene from the extreme halophyte *Salicornia brachiata* enhances Na^+ loading in xylem and confers salt tolerance in transgenic tobacco. *BMC Plant Biology* **12,** 188.

Yang L., Ma C., Wang L., Chen S. & Li H. (2012) Salt stress induced proteome and transcriptome changes in sugar beet monosomic addition line M14. *Journal of Plant Physiology* **169,** 839–850.

Yin L., Wang S., Eltayeb A.E., Uddin M.I., Yamamoto Y., Tsuji W., . . . Tanaka K. (2010) Overexpression of dehydroascorbate reductase, but not monodehydroascorbate reductase, confers tolerance to aluminum stress in transgenic tobacco. *Planta* **231,** 609–621.

Yu J., Chen S., Zhao Q., Wang T., Yang C., Diaz C., . . . Dai S. (2011) Physiological and proteomic analysis of salinity tolerance in *Puccinellia tenuiflora*. *Journal of Proteome Research* **10,** 3852–3870.

Zhang H., Han B., Wang T., Chen S., Li H., Zhang Y. & Dai S. (2011) Mechanisms of plant salt response: insights from proteomics. *Journal of Proteome Research* **11,** 49–67.

Zhang H., Zhang L., Lv H., Yu Z., Zhang D. & Zhu W. (2014) Identification of changes in *Triticum aestivum* L. leaf proteome in response to drought stress by 2D-PAGE and MALDI-TOF/TOF mass spectrometry. *Acta Physiologiae Plantarum* **36,** 1385–1398.

Zhang Y., Lai J., Sun S., Li Y., Liu Y., Liang L., . . . Xie Q. (2008) Comparison analysis of transcripts from the halophyte *Thellungiella halophila*. *Journal of Integrative Plant Biology* **50,** 1327–1335.

Zhu J. (2000) Genetic analysis of plant salt tolerance using Arabidopsis. *Plant Physiology* **124,** 941–948.

Zhu J. (2001) Plant salt tolerance. *Trends in Plant Science* **6,** 66–71.

Received 26 March 2014; received in revised form 19 July 2014; accepted for publication 23 July 2014

SUPPORTING INFORMATION

Additional Supporting Information may be found in the online version of this article at the publisher's web-site:

Figure S1. 2-DE patterns in the leaf proteins of *Halogeton glomeratus*. Two months old seedlings were treated with 200 mM NaCl for 0 h (A), 24 h (B), 72 h (C) and 7 d (D). 2-DE patterns were shown 3 biological replicates.

Table S1. Protein spots with significantly changed relative abundances in leaves of *Halogeton glomeratus*. The protein spots shown in Fig. 5 were quantified using PDQuest software (Bio-Rad). Results are presented as the mean ± SE of relative protein intensity for gels from 3 biological replicates. The *P*-value shows significant changes in abundance level according to the t-test through analysis of variance ($P < 0.05$).

Table S2. Peptide sequence data for the 49 protein spots identified by MALDI-TOF/TOF MS/MS. This table presents analytical details for the proteins listed in Table 1. Spot numbering refers to Fig. 5. MS/MS data were interpreted using MASCOT (http://www.matrixscience.com) program searching the EST database of *Halogeton glomeratus*.

Appendix S1. The detail information of nucleotide sequence and coding region sequences (CDS) of unigenes in EST database of *Halogeton glomeratus*.